High power density laser estimation using quantitative thermal imaging method

Abderezak Aouali, Thomas Lafargue-Tallet, Stéphane Chevalier, Alain Sommier, Raymond Peiffer, Maximilian Taillandier, Jean-Christophe Batsale, Christophe Pradere

High power density laser estimation using quantitative thermal imaging method

Abderezak Aouali[a], Thomas Lafargue-Tallet[b], Stéphane Chevalier[a], Alain Sommier[a], Raymond Peiffer[b], Maximilian Taillandier[b], Jean-Christophe Batsale[a] and Christophe Pradere[c]

[a]TREFLE, I2M TREFLE, UMR 5295 CNRS-UB-ENSAM, Talence, France; [b]Aérodynamique Propulsion et Létalité, MBDA France, Le Plessis-Robinson, France; [c]R&D, EPSYL-Alcen, Talence CEDEX, France

ABSTRACT

The knowledge of the amplitude and the spatial distribution of an excitation flux is of great interest for the quantification of heat sources. In this work, the development of a non-contact imaging powermeter based on the association of a bolometer with an infrared camera is described. This powermeter allows, thanks to infrared thermographic measurements and image processing methods, the quantitative estimation of the spatial distribution of the power of the flux delivered by a high-power laser. First, the experimental setup used is described. Then, the complete modelling of the heat transfer within the bolometer using the 3D thermal quadrupole formalism is presented. After that, an inverse method based on the Wiener filter in Fourier-Laplace transform spaces to estimate the spatial distribution of the power flux is described. Finally, power estimation results using two metallic plates as a bolometer are presented and discussed.

ARTICLE HISTORY

Received 6 April 2023
Accepted 20 June 2023

KEYWORDS

IR thermography; thermal inverse methods; fluxmetry

1. Introduction

The knowledge of the heat flux generated by a source is of primary interest in many scientific fields. For example, in the fields of building science, aeronautics, optical applications or heat transfer, the access to the quantitative heat flux field is an input for many mutiphysical problems and can be of prior interest to control or monitor online processes. In this context, the development of a quantitative and imaging powermeter implies, on the one hand, to develop the sensitive component which will absorb the radiation of the source excitation (bolometer), and on the other hand, to establish the mathematical model which describes the heat transfer within the bolometer in order to guarantee the quantitative aspect of the powermeter.

There are two main types of flux sensors: thermal sensors and photonic sensors. Photonic sensors are based on the photoelectric effect and are mainly used at higher frequencies in the visible, ultraviolet and X-ray spectral range. In contrast, thermal sensors are mainly used at longer wavelengths [1–3]. In this study, the choice of material is metallic plates that act as

CONTACT Abderezak Aouali abderezak.aouali@u-bordeaux.fr TREFLE, I2M TREFLE, UMR 5295 CNRS-UB-ENSAM, 351 Cours de la Libération, Talence 33400, France

a deported bolometer and can withstand the impact of high flux. The metallic plates absorb electromagnetic radiations upon impact and subsequently heat up, making the thermal scene visible by an IR camera. However, to obtain a quantitative image of the heat flux, or the thermal source that excites the bolometer, extensive mathematical processing based on inverse thermal methods is required.

There are several methods in the literature to estimate the heat sources according to the nature of the heat transfer [4–6]. In the present study, the reconstruction of the heat sources is mainly based on the knowledge of the heat transfer by conduction. In the work from Garderein et al. [7], a point sensor system based on a thermocouple has been developed to estimate local fluxes based on analytical inverse thermal methods. Another study from Zeribi et al. [8] reports the fabrication of a 2D non-imaging heat flux sensor based on the spatial temperature gradient method. Image reconstructions were tackled in the work from Groz et al. [9,10] who reported a method to reconstruct heat sources using analytical models and two inversion methods (statistical and deconvolution by Toeplitz). Another 3D reconstruction method was recently developed by P. Burgholzer et al. [11,12]. This method combines infrared thermography and the concept of virtual waves. However, in these studies, the quantitative aspect of the heat flux power estimating was not reached. Furthermore, in the study realised by Aouali et al. [3], a quantitative imaging powermeter based on a hyperspectral thermoconverter has been developed using EMIR technology [13]. However, this powermeter is not adapted for high flux application. Finally, the work of Nortershauser et al. [14,15] focused on the development of a source reconstruction method (spatial distribution and flux power) using numerical inversion models. The constraint of this method is mainly related to the computation time; however, the authors propose the use of a statistical estimator in the Fourier transform space in order to win in computation time. From all these precursory works, the development of a method of quantitative estimation of high fluxes coupled with an imaging bolometer would allow the design of an imaging and quantitative powermeter adapted to extreme conditions.

The present work reports the development of a contactless imaging fluxmeter for high density power flux estimation. To the author's best knowledge, such a sensor based on a metallic plate and analytical inverse method for the estimation of the quantitative and spatial cartography of heat sources has not been reported in the literature. To tackle this objective, the heat transfer within a metallic plate is modelled. Next, the method used for the mathematical processing of the images acquired by the IR camera is presented. Finally, two examples of source reconstruction using two different metallic plates are presented and discussed.

2. Experimental setup

The experimental set-up is shown in Figure 1, a very high-power laser source developed by ALPhANOV[1] with adjustable output power between $0-10$ KW (with an uncertainty estimated at 2% by the manufacturer) and response time of 50 ms is used. The use of powerful lasers can be very dangerous and requires rigorous safety precautions. This is why the entire assembly is placed in a secure enclosure called a laser protection cage (dimensions: 5m $\times$ 2.4m $\times$ 2.6m) which is covered with a protective foam ensuring 30 s of resistance to a 10 kW laser flux. The interior of the cage is also covered with numerous sensors and active panels that allow an emergency stop to be triggered if they are

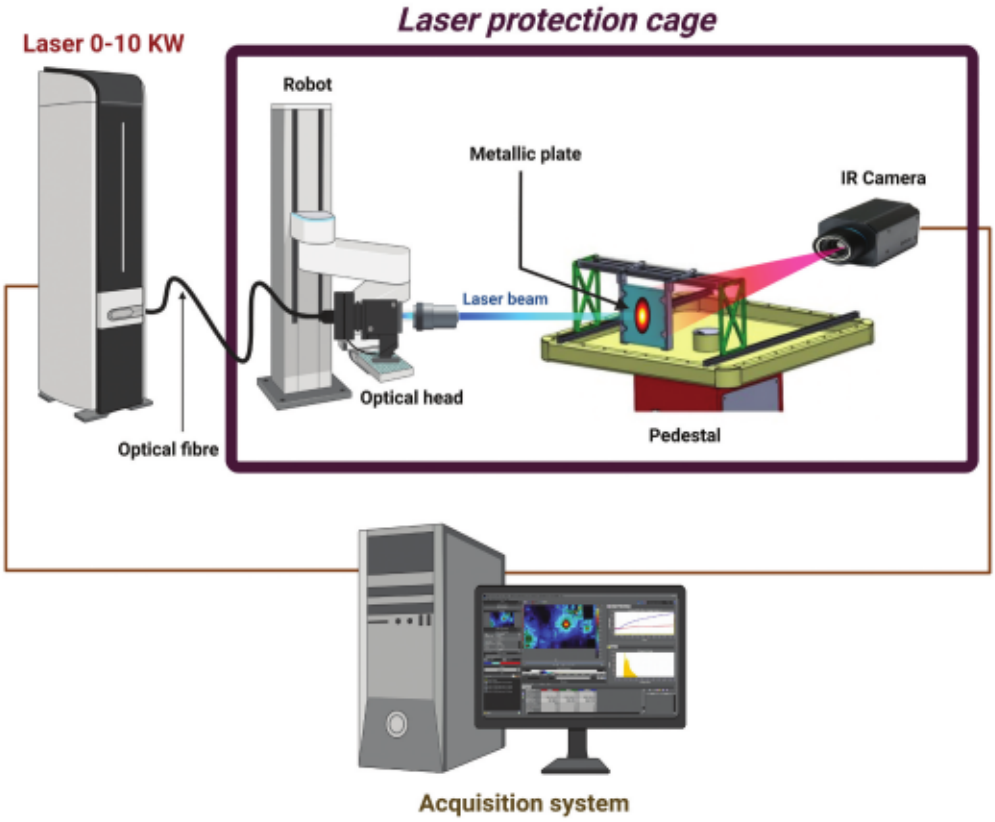

Figure 1. Experimental setup.

subjected to laser illumination, only the laser cabinet and acquisition system is kept outside the cage. The laser source delivers a Gaussian laser beam with a wavelength of $\lambda_m = 1070$nm and variable power according to the setpoint. The beam is conveyed by an optical fibre of 200μm diameter to the optical head, the optical head is composed of different optical elements (objective, lenses. . .) which allow to modify the path and the size as well as to collimate the laser beam. The optical head rests on a robot that allows the beam to be directed with a normal incidence to impact the target (metallic plate). Finally, a FLIR InSb SC 7000 IR camera (working in the spectral range [1.5 μm-5.5 μm] with a sensor of 240 $\times$ 320 pixels and a pitch size of 25 μm/px) placed behind the metallic plate is used to make the acquisitions. The metallic plate is painted black on its front and back face in order to be assimilated to a black body ($\varepsilon \approx 1$) and to avoid the reflection of the laser beam on the front face (total transmission). In this study, measurement in transmission mode is preferred to reflection mode for reasons of space requirements and safety in the cabin in view of the high power delivered by the laser (risk of damaging the IR camera).

3. Heat transfer modelling in a homogeneous metallic plate

Consider a homogeneous and isotropic plate of dimensions $L_x \times L_y \times e(\mathrm{m})$, diffusivity $a(\mathrm{m}^2.\mathrm{s}^{-1})$ and thermal conductivity $\lambda(\mathrm{W.m}^{-1}.\mathrm{K}^{-1})$. Suppose that at $t = 0$, a heat source

from a laser beam thermally excites the front face of the plate. In order to simplify the boundary conditions, the plate is assumed to be adiabatic on the lateral faces (see Figure 2). The associated 3D problem for the temperature calculation $T(\mathrm{K})$ can be written as follows:

$$\begin{cases} \frac{1}{a}\frac{\partial T(x,y,z,t)}{\partial t} & = & \frac{\partial^2 T(x,y,z,t)}{\partial x^2} + \frac{\partial^2 T(x,y,z,t)}{\partial y^2} + \frac{\partial^2 T(x,y,z,t)}{\partial z^2} \\ -\lambda \frac{\partial T(x,y,z,t)}{\partial x}\Big|_{x=0,L_x} & = & 0 \\ -\lambda \frac{\partial T(x,y,z,t)}{\partial y}\Big|_{y=0,L_y} & = & 0 \\ -\lambda \frac{\partial T(x,y,z,t)}{\partial z}\Big|_{z=0} & = & -h_c\, T(x,y,z=0,t) + \phi(x,y,t) \\ -\lambda \frac{\partial T(x,y,z,t)}{\partial z}\Big|_{z=e} & = & h_c\, T(x,y,z=e,t) \\ T(x,y,z,t=0) & = & 0 \end{cases} \tag{1}$$

where ϕ is the power density, expressed in $\mathrm{W.m^{-2}}$.

3.1. Resolution of the problem

One way of solving Equation (1) is to write it in the Laplace and Fourier-cosine domains. Indeed, the application of a Laplace transform in time and two Fourier-cosine transforms in space to the temperature field $T(x,y,z,t)$ is defined as follows:

$$\theta(a_n,\beta_m,z,p) = \int_0^{L_x}\int_0^{L_y}\int_{t=0}^{+\infty} T(x,y,z,t)e^{-pt}\cos(a_n x)\cos(\beta_m y)\; dt\; dy\; dx, \tag{2}$$

where $a_n = \frac{n\pi}{L_x}$, $n \in \mathbb{N}$ and $\beta_m = m\pi/L_y$, $m \in \mathbb{N}$ represent the spatial Fourier frequencies. In order to solve Equation 1 in the Laplace-Fourier transformed space, the

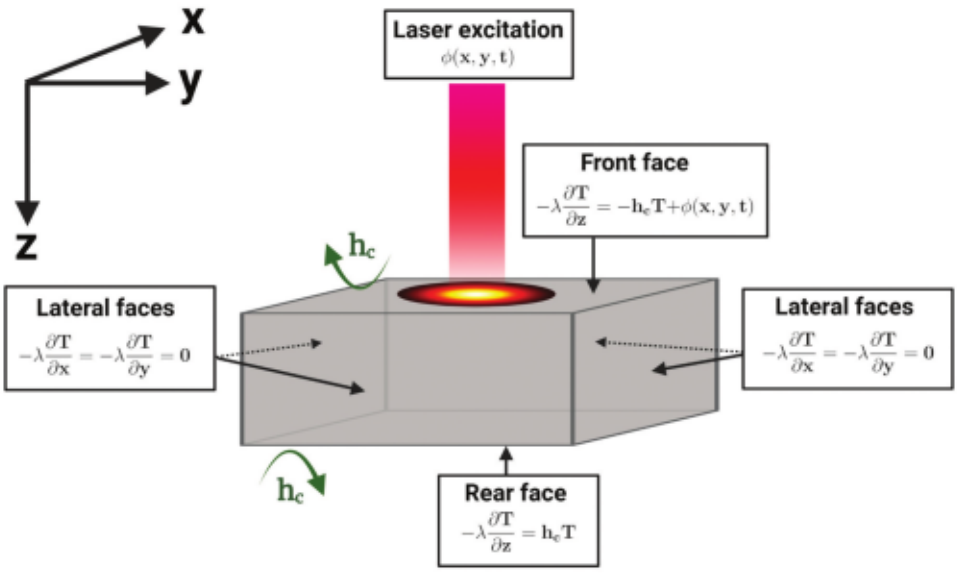

Figure 2. Heat transfer in a homogeneous medium.

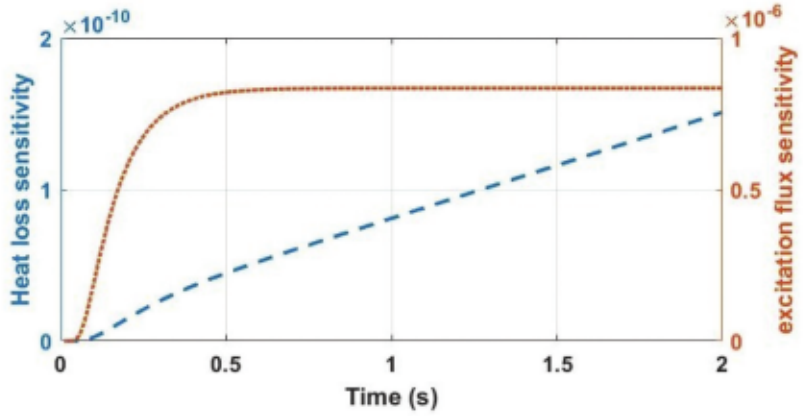

Figure 3. Model sensitivity, (a) Heat losses sensitivity, (b) Excitation flux sensitivity.

thermal quadrupole formalism [16] has been used. The principle of the method is described in the first part of the book. The resolution of the system is obtained as follows:

$$\begin{bmatrix} \theta_{m,n}(z=0,p) \\ \varphi_{mn}(p) - h_c\,\theta_{m,n}(z=0,p) \end{bmatrix} = \begin{bmatrix} A_{m,n} & B_{m,n} \\ C_{m,n} & D_{m,n} \end{bmatrix} \times \begin{bmatrix} \theta_{m,n}(z=e,p) \\ h_c\,\theta_{m,n}(z=e,p) \end{bmatrix}, \tag{3}$$

with,

$$\begin{bmatrix} A_{m,n} & B_{m,n} \\ C_{m,n} & D_{m,n} \end{bmatrix} = \begin{bmatrix} \cosh(e\,\xi_{m,n}) & \sinh(e\,\xi_{m,n})/(\lambda\,\xi_{m,n}) \\ \lambda\,\xi_{m,n}\sinh(e\,\xi_{m,n}) & \cosh(e\,\xi_{m,n}) \end{bmatrix}, \tag{4}$$

and,

$$\xi^2 = \left(\alpha_n^2 + \beta_m^2 + \frac{p}{a}\right), \tag{5}$$

Hence, the expression of the temperature in the rear face of the material is given by:

$$\theta_{m,n}(z=e,p) = \frac{\varphi_{m,n}(p)}{C_{m,n} + 2h_c\,A_{m,n} + h_c^2\,B_{m,n}}, \tag{6}$$

In order to obtain the temperature field in real-time space, two inverse cosine transformations in space and one inverse Laplace transformation in time are required. From Equation 6, the point source impulse response $\delta(x,y,t)$ in the rear face of the material in Fourier-Laplace transformed space is written as follows:

$$H_{m,n}(z=e,p) = \frac{1}{C_{m,n} + 2h_c\,A_{m,n} + h_c^2\,B_{m,n}}, \tag{7}$$

Identifying the analytical expression of the point source impulse response is an important step in this study. Indeed, it makes it possible to calculate the temperature of a homogeneous material for any spatial and temporal form of the excitation.

From the analytical solution (Equation 7), the sensitivity of the model to different parameters can be established. Figure 3 shows the sensitivity of the model to the excitation flux and to the heat losses; it appears that the heat losses appear a little later

and with a much lower sensitivity than the heat flux. It is therefore concluded that the heat losses can be neglected during the estimation of the excitation flux assuming that short times are used in the processing.

4. Description of the inverse method for flux estimation

Based on Equation 6, the output temperature can simply be written as a space-time convolution product between the excitation source and the source point impulse response:

$$T(x,y,z=e,t) = \mathcal{Y}(x,y,z=0,t) \circledast \widehat{h}(x,y,z=e,t), \tag{8}$$

Where $\hat{h}(x,y,t)$ is the point source impulse response in real space-time. The source $\mathcal{Y}(x,y,t)$ can be decomposed into a product of a spatial function $\mathcal{F}(x,y)$, a peak power $\mathcal{Y}_0$ and a temporal function $\Theta(t)$. After passing through the space transformed cosine base, only the temporal convolution remains. In the case of a Heaviside-type temporal excitation, and after applying the Laplace transform on time, we have:

$$\theta(a_n,\beta_m,z=e,p) = \mathcal{Y}_0 \times \widehat{\mathcal{F}}(a_n,\beta_m) \times \underbrace{\left[\frac{1}{p} \times H(a_n,\beta_m,z=e,p)\right]}_{H^{\Theta}}, \tag{9}$$

Where H^{Θ} represents the point source response to the Heaviside temporal excitation in Laplace-cosine transformed space. By applying the Laplace inverse transform to Equation 9, the source can be estimated in the cosine transformed space via the following relation:

$$\mathcal{Y}_0 \times \hat{\mathcal{F}}(a_n,\beta_m) = \hat{\theta}(a_n,\beta_m,z=e,t) \times \left[\hat{H}^{\Theta}(a_n,\beta_m,z=e,t)\right]^{-1}, \tag{10}$$

Inverse thermal problems are known to be ill-posed problems [17]. This is essentially due to the condition of instability of the solution obtained by inversion. To remedy this condition, the inversion is carried out by constructing a Wiener filter. This filter is based on Tikhonov's regularisation method [18], which is used and applied in the cosine transformed space as follows:

$$\mathcal{Y}_0 \times \widehat{\mathcal{F}}(a_n,\beta_m) = \widehat{\theta}(a_n,\beta_m,z=e,t) \times \frac{\widehat{H}^{\Theta}(a_n,\beta_m,z=e,t)}{\left|\widehat{H}^{\Theta}(a_n,\beta_m,z=e,t)\right|^2 + \mu\left|\widehat{D}(a_n,\beta_m)\right|^2}, \tag{11}$$

Where D is a derivation matrix [19] in the cosine transformed space and μ is the regularisation coefficient [20]. In the end, to retrieve the spatial distribution of the source, two inverse cosine transformations are necessary. The optimal value of the regularisation coefficient is determined by the analysis of the singular values after applying an SVD transform [21].

5. Results and discussion

In this section, the inverse method was applied using two metallic plates (aluminium and copper) painted black (so that the emissivity is closed to the one of a black body $\varepsilon \approx 1$). The thickness of the plates was chosen to take into consideration the characteristic thermal diffusion time in order to have a usable signal on the rear face measurement.

The laser is set to deliver a Gaussian beam of diameter $d = 20$mm and a power set point of $P = 1$kW. The IR camera was placed in the rear face of the metallic plate to make acquisitions at a frequency of $f = 100$Hz. The point source response to the Heaviside temporal excitation was calculated in both cases, and the excitation flux field was estimated using Equation 11.

5.1. Case of an aluminium metallic plate

In this first application, a homogeneous aluminium metallic plate with spatial dimensions 10 cm × 10 cm × 1 cm, and thermal properties of diffusivity $a = 9.88 \times 10^{-5}\mathrm{m^2s^{-1}}$, conductivity $\lambda = 237\,\mathrm{Wm^{-1}K^{-1}}$ has been used. The pixel size in this case is equal to $L_{pix} = 540\,\mu$m.

The absolute temperature field measured at the rear face is shown in Figure 4.

Figure 4(a) shows the diffusion of the 2D temperature field during times. Figure 4(b) shows the evolution of the relative temperature of the central pixel as a function of time, and it can be seen that the relative temperature reaches almost 100K in less than 2s, this is likely to modify the thermophysical properties of the aluminium plate (thermodependence of the thermophysical properties [22,23]). To remedy this and to keep the problem linear, the temperature at the front of the plate was calculated using the quadrupole thermal model in order to have an approximation of the temperature rise; thus, only the part lower than 50K ($t = 0.75$s) will be exploited. Figure 4(c) shows the normalised plane diffusion of the midline over time, it can be seen that the heat diffusion does not reach the edges of the metallic plate, which confirms the assumption of adiabatic conditions at the edges during the modelling of the heat transfer regarding the plate size of 10 cm at all.

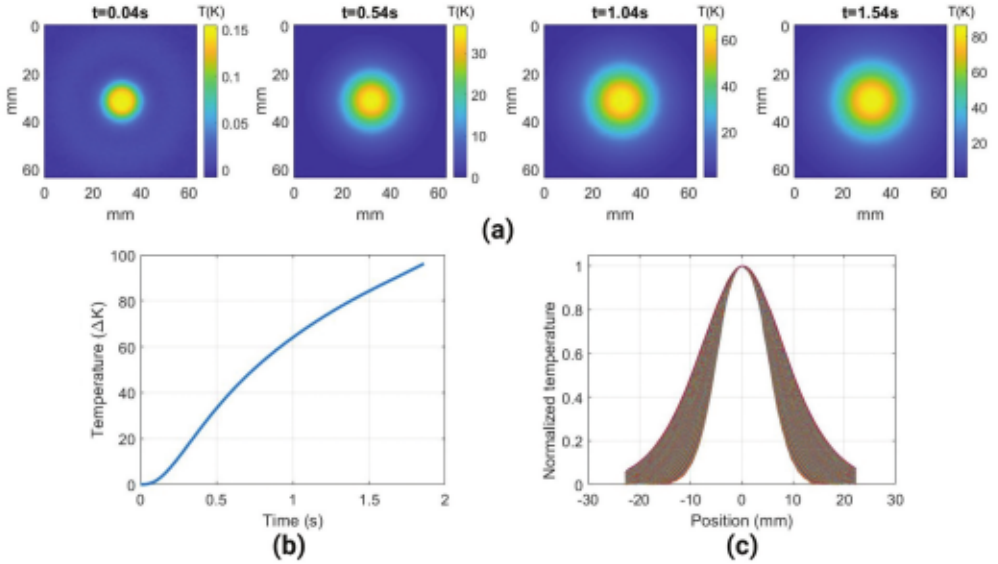

Figure 4. Region of interest of the absolute temperature field measured at the rear face of the plate: (a) spatial temperature field diffusion chronogram, (b) central pixel temperature evolution over time, (c) normalized plane diffusion of the midline over time.

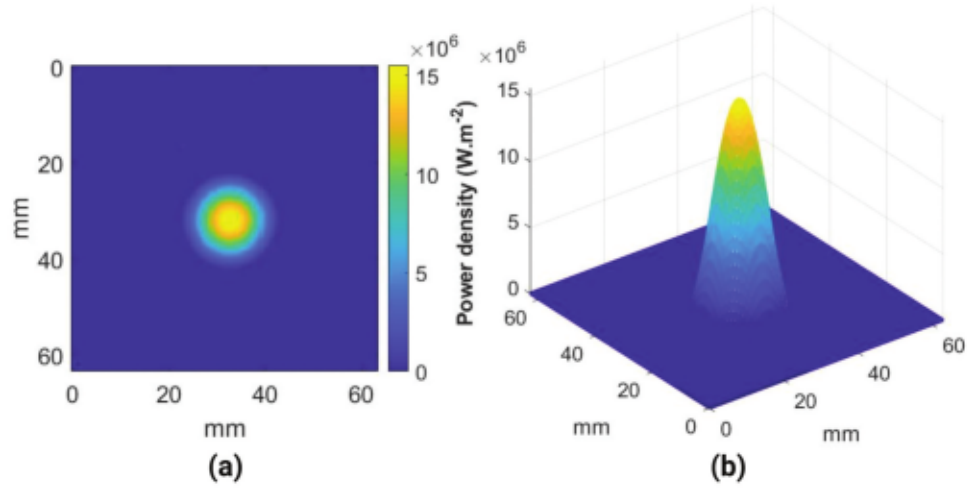

Figure 5. (a) image of the estimated source and (b) surfacing of the estimated source.

Figure 5(a,b) show the reconstruction of the spatial distribution and power density of the excitation flux after application of the inverse method. In order to determine the global injected power, two methods are possible: (i) multiply the imaged flux density by the area and then integrate it or (ii) integrate the flux density image and multiply the result by the area of a pixel. by Applying the second method, the estimated power is:

$$P_{\text{estimated}} = \left(\iint \mathcal{Y}(x,y) \right) \times S_{pixel} = 977 \pm 32, \tag{12}$$

Where: S_{pixel}: area of a pixel which is equal to $2.916 \times 10^{-7}\text{m}^2$. The estimated power represents a relative error of: 2.26% in respect of the laser's set power.

The uncertainty in the estimated global power is calculated overall and takes into account the uncertainties relating to thermophysical properties, measurement of temperature fields and estimation by the inverse method and the choice of the regularisation coefficient. In addition, this overall uncertainty is obtained by calculating the standard deviation on the result of the global power estimated as a function of time after reaching the set power. The same approach will be used in the case of the copper metallic plate.

In order to calculate the estimated excitation flux diameter and compare it to the theoretical beam diameter delivered by the laser, three steps are necessary. Firstly, the centre line of the estimated source image is identified and plotted. Secondly, using linear least squares minimisation, the Gaussian function corresponding to the plotted centerline is identified. Finally, and by definition [24], the diameter of the Gaussian corresponds to four times its standard deviation ($d_{\text{estimated}} = 4 \times \sigma$).

Figure 6 shows the plot of the centre line of the source image and the function obtained by the minimisation. The function obtained is expressed as follows:

$$f(x) = \exp\left(\frac{-x^2}{2\sigma^2}\right) \Rightarrow \sigma = 5 \pm 0.008 \times 10^{-3}\text{m}, \tag{13}$$

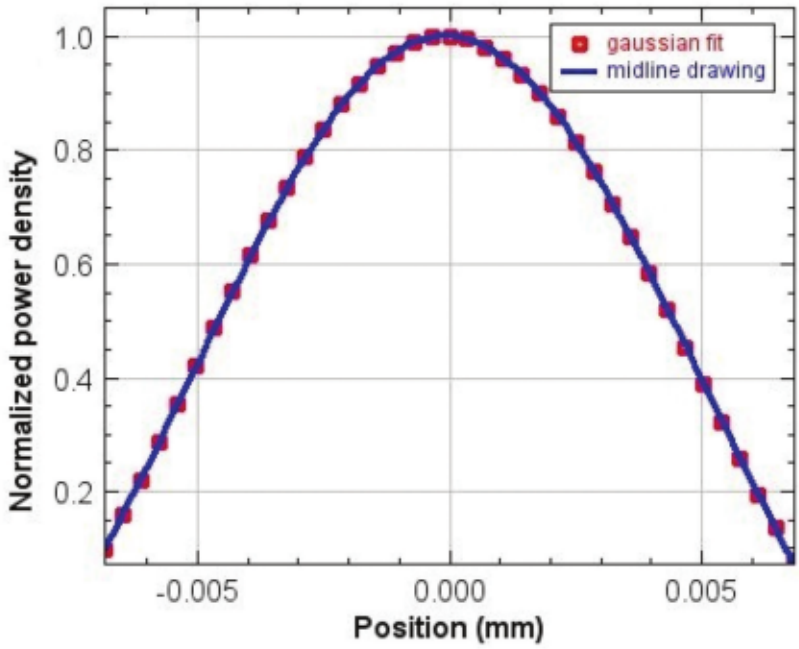

Figure 6. Linear least squares median line minimisation of the estimated source image.

From Equation 13, the estimated Gaussian beam diameter is: $d_{\text{estimated}} = 4 \times \sigma = 2 \pm 0.0032 \times 10^{-2}$m with an error relative to the target diameter ($d = 2 \times 10^{-2}$ m) equal to 0.16%.

5.2. Case of a copper metallic plate

In this second application, a homogeneous copper metallic plate with spatial dimensions (10cm $\times$ 10cm $\times$ 2cm) and thermal properties of diffusivity $a = 1.17 \times 10^{-4}\text{m}^2\text{s}^{-1}$ and conductivity $\lambda = 400\text{Wm}^{-1}\text{K}^{-1}$ has been used. The pixel size in this case is of the order of $L_{pix} = 360\mu$m.

The absolute temperature field measured is shown in Figure 7. Figure 7(a) shows the evolution of the 2D temperature field diffusion at different times. It should be noted that the temperature field measured at $t = 0.04$ s is on average around 0.02 K, which corresponds more to the noise measurement as well as the error resulting from the subtraction of the first image in order to evaluate only the temperature difference. Figure 7(b) shows the evolution of the temperature of the central pixel as a function of time, and it can be seen that the relative temperature reaches approximately 12 K after 2 s of excitation. Therefore, the heat diffusion effects can be considered linear and the 2 s of experimental time are fully exploitable (the temperature at the front side was also calculated using the thermal model as in the case of the aluminium plate). On the other hand, due to the significant thickness of the material and its high diffusivity, short times will be preferred during processing. Figure 7(c) shows the normalised plane diffusion of the midline over time and confirms the adiabatic condition assumption at the edges of the plate during the heat transfer

modelling. It can be seen in this figure that the curves measured at short times are noisy in contrast to the case of the aluminium plate, this is due to the fact that the plate is twice as thick, and therefore the diffusion characteristic time is greater (3.4 s in this case).

Figure 8(a,b) show the reconstruction of the spatial distribution and power density of the excitation flux. After applying the inverse method, the estimated power using Equation12 was found to be 1010.6 ± 3.7W ($S_{pixel} = 1.296 \times 10^{-7}$m) with a relative error of 1.05% in respect of the laser's set power. As previously, the midline of the

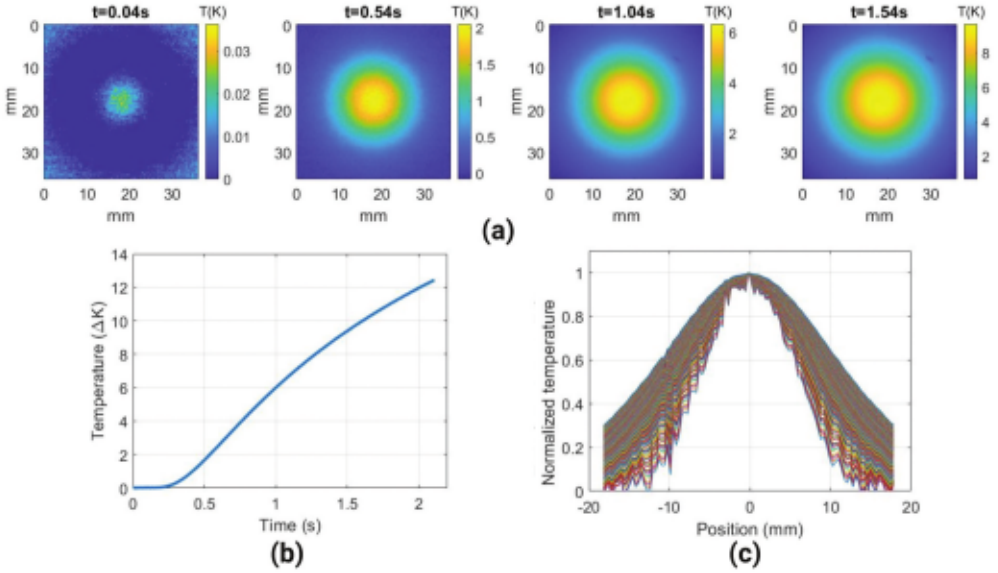

Figure 7. Region of interest of the absolute temperature field measured at the rear face of the plate: (a) spatial temperature field diffusion chronogram, (b) central pixel temperature evolution over time, (c) normalized plane diffusion of the midline over time.

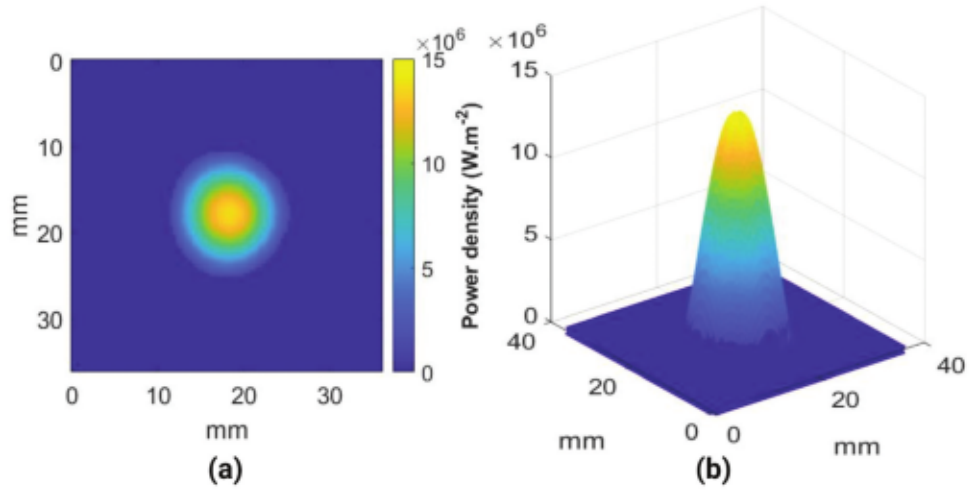

Figure 8. (a) Image of the estimated source and (b) surfacing of the estimated source.

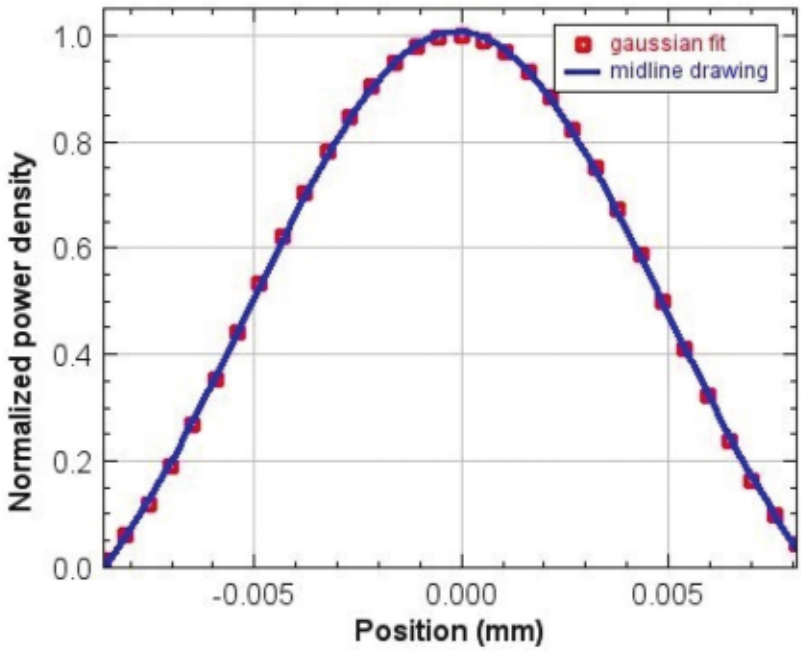

Figure 9. Linear least squares median line minimisation of the estimated source image.

estimated source image is identified and plotted, then, the Gaussian function corresponding to the plotted midline is identified using linear least squares minimisation.

Figure 9 shows the plot of the centre line of the source image and the function obtained by the minimisation. The function obtained is expressed as follows:

$$f(x) = \exp\left(\frac{-x^2}{2\sigma^2}\right) \Rightarrow \sigma = 5 \pm 0.083 \times 10^{-3}\text{m}, \tag{14}$$

From Equation 14, the estimated Gaussian beam diameter is: $d_{\text{estimated}} = 4 \times \sigma = 2 \pm 0.033 \times 10^{-2}$m with a relative error equal to 1.63%.

6. Conclusion

A powermeter using a metallic converter associated with an IR bolometric camera was used to estimate the spatial distribution of high-power optical fluxes.

The most important point is the experimental validation of the thermoconverter and infrared camera configuration. Firstly, the development of a thermal model to precisely characterise the heat transfer within the bolometer was described. Then, an inverse method was used to estimate the spatial reconstruction of sources and their flux density.

The methodology was applied using a high-power laser, and the quantitative spatial power density of the excitation flux was estimated using two metallic plates (copper and aluminium) as bolometer. The flux density and spatial distribution were estimated with a relative error of 2.26% and 1.05%, respectively.

This research offers new perspectives in the fields of high flux estimation and thermal inverse methods, with many applications projected in the fields of optical applications, building science and industries.

Note

1. https://www.alphanov.com (2023).

Acknowledgements

This research is part of IGAR project that aims to thermally and chemically characterise plasma torches. The main challenge is the contactless 3D temperature and flux field measurement for energy optimisation of these torches.

The authors would like to thank ADEME for the support of his work through the IGAR project with Arcelor-Mittal.

Disclosure statement

No potential conflict of interest was reported by the author(s).

Funding

ADEME through IGAR project with Arcelor-Mittal.

Notes on contributors

Abderezak Aouali received his PhD degree mechanics from the University of Bordeaux (FRANCE) in 2022, he worked on the energy optimization of plasma torches within the institute of mechanics and engineering (I2M). Between 2022 and 2023 he was a postdoctoral fellow. His areas of interest cover multiscale and multiphysical characterization of materials, non-destructive testing, heat and masse transfer under extreme temperature and flux conditions.

Thomas Lafargue-Tallet received his PhD degree mechanics from the Arts et Métiers Institute of Technology (ENSAM, Bordeaux) in 2023, he worked on the behavior of materials illuminated by high-power laser sources within the Institute of Mechanics and Engineering (I2M) in collaboration with MBDA France. His areas of interest cover laser vulnerability, conducto-radiative transfers in materials.

Stéphane Chevalier After a PhD from Nantes Université on thermal fuel cell diagnostic by electrochemical impedance spectroscopy, he has joined the TEAM labs at University of Toronto for a postdoctoral position. In 2016, he was awarded by a Marie Currie fellowship to return in France for a second postdoc position. From 2018, he works as Associate Professor at I2M and Arts et Métiers Institute of Technology with research field in energy transfer characterizations in microsystems using multispectral IR imaging.

Alain Sommier received his PhD degree in Ingineer Science from the Nantes University in 1998. Between 1998 and 2008, he worked in food process (INRA and AgroParisTech) to study heat and mass transfer in alimentary products. He is currently a research ingineer (CNRS) at Mechanical et Engineering Institute I2M in Bordeaux University, France. His areas of interest cover heat and mass transferts, thermal characterization, non destructive testing and non destructive evaluation based on transient thermal field analysis.

Raymond Peiffer, PhD in 1978, works for the Industry since 1979 on multi-physics and multi-domains subjects, including technics and technological aspects.

Maximilian Taillandier is a trained mechanical engineer (ETH Zürich) and has an aerospace engineering degree from ISAE-SUPAERO. Since 2016 he works at MBDA in France in the missile design directorate.

Jean-Christophe Batsale was born in 1959 in Bordeaux (France). He obtained a PhD in Mechanical Engineering at the University of Bordeaux in 1984 and a Capacitation to Steer Researches (Habilitation à Diriger des Recherches) at the Institut National Polytechnique de Lorraine, Nancy, (France) in 1992. He became Senior Scientist (Chargé de recherche), in 1985, at the french center for research: « Centre National de la Recherche Scientifique » (CNRS) at the Laboratoire d'Energétique et de Mécanique Théorique et Appliquée, in Nancy. He returned to Bordeaux in 1995 as Senior Scientist at the Laboratoire Energétique et Phénomènes de Transfert. Since 1998, he is Professor in the Bordeaux Campus at the school of engineering: "Arts et Métiers Paris-Tech" (In charge for pedagogy of the "heat and mass transfer" department and affected at the I2M-Institute of Mechanics and Mechanical engineering, Joint Research Unit CNRS 5295, head of the "transfer and fluids" research department). His research fields are related to the measurement of thermophysical properties of heterogeneous media and energetic systems based on the analysis of transient temperature responses to a calibrated heating. The design of such instruments is very often based on infrared thermography and optical devices, but also contact sensors and contact heating devices. From the beginning, these instruments were associated to the development of data processing methods (inverse methods related to modelling of heat transfer in heterogenous media, quadrupole methods, homogenization, integral transform…). These methods have been applied to industrial domains such as: materials (composite, ceramics), chemical engineering, optics, food industry…

Christophe Pradere After a PhD at ENSAM-PARISTECH School on thermal characterization of carbon fiber at very high temperature, he has joined the SOLVAY group for a post-doctoral position in order to study the heat and mass transfer in microfluidic reactive system by InfraRed thermography. From 2006 to 2021, he was a French CNRS researcher at I2M institute with research field around heterogeneous thermal system of energy conversion by using multispectral IR imaging. Since 2021, he has joined a private company to develop the field of InfraRed Quantitative Non Destructive Testing (QNDT EPSYL) in industrial applications.

ORCID

Abderezak Aouali http://orcid.org/0000-0003-0672-1960

References

[1] Pradere C, Caumes JP, Balageas D, et al. Photothermal converters for quantitative 2d and 3d real-time terahertz imaging. Quant Infrared Thermogr J. 2010;7(2):217–235. doi: 10.3166/qirt.7.217-235

[2] Müller R, Bohmeyer W, Kehrt M, et al. Novel detectors for traceable thz power measurements. J Infrared Milli Terahz Waves. 2014;35(8):659–670. doi: 10.1007/s10762-014-0066-z

[3] Aouali A, Chevalier S, Sommier A, et al. Ultra-broadband contactless imaging power meter. Appl Opt. 2021;60(26):7995–8005.

[4] Gidik H, Dupont D, Bedek G. Development of a radiative heat fluxmeter with a textile substrate. Sens Actuators A. 2018;271:162–167. doi: 10.1016/j.sna.2017.12.020

[5] Jim CY, Hongming H. Estimating heat flux transmission of vertical greenery ecosystem. Ecol Eng. 2011;37(8):1112–1122. doi: 10.1016/j.ecoleng.2011.02.005

[6] Yang K, Wang J. A temperature prediction-correction method for estimating surface soil heat flux from soil temperature and moisture data. Sci China Ser D-Earth Sci. 2008;51(5):721–729. doi: 10.1007/s11430-008-0036-1
[7] Gardarein JL, Battaglia JL, Lohle S, et al. Miniaturized heat flux sensor for high enthalpy plasma flow characterization. Inverse Prob Sci Eng. 2013;21(4):605–618. doi: 10.1080/17415977.2012.712525
[8] Zribi A, Barthès M, Bégot S, et al. Design, fabrication and characterization of thin film resistances for heat flux sensing application. Sens Actuators A. 2016;245:26–39. doi: 10.1016/j.sna.2016.04.040
[9] Groz MM, Abisset-Chavanne E, Meziane A, et al. Bayesian inference for 3d volumetric heat sources reconstruction from surfacic ir imaging. Appl Sci. 2020;10(5):1607. doi: 10.3390/app10051607
[10] Groz MM, Abisset-Chavanne E, Meziane A, et al. Three- dimensional reconstruction of thermal volumetric sources from surface temperature fields measured by infrared thermography. Appl Sci. 2019;9(24):5464. doi: 10.3390/app9245464
[11] Burgholzer P, Thor M, Gruber J, et al. Three-dimensional thermographic imaging using a virtual wave concept. J Appl Phys. 2017;121(10):105102. doi: 10.1063/1.4978010
[12] Waters S, Burgholzer P, Mendioroz A, et al. 3d reconstruction of tilted cracks using infrared thermography and the virtual wave concept. In: Proceedings of the 14th International Conference on Quantitative Infrared Thermography, Berlin, Germany; 2018. p. 25–29.
[13] Balageas D, Levesque P, Deom A. Characterization of electromagnetic fields using a lock-in infrared thermographic system. In Thermosense XV: An International Conference on Thermal Sensing and Imaging Diagnostic Applications, Vol. 1933, Orlando, FL, US: International Society for Optics and Photonics; 1993. p. 274–285.
[14] Nortershauser D, Millan P. Resolution of a three-dimensional unsteady inverse problem by sequential method using parameter reduction and infrared thermography measurements. Numer Heat Transfer: Part A: Applications. 2000;37(6):587–611.
[15] Nortershauser D, Millan P. Estimation of moving heat sources with a three- dimensional unsteady inverse method. Aerosp Sci Technol. 2001;5(8):529–540. doi: 10.1016/S1270-96380101130-0
[16] Maillet D, André S, Batsale JC, et al. Thermal quadrupoles, solving the heat equation through integral transforms. New York, US: John Wiley & Sons Incorporated; 2000.
[17] Hadamard J. Lectures on cauchy's problem in linear partial differential equations. New Haven: Yale University Press; 1923;12(171):173–174.
[18] Tikhonov AN. On the solution of ill-posed problems and the method of regularization. Russ Acad Sci. 1963;3(151):501–504.
[19] Gray RM. Toeplitz and circulant matrices: a review. Found Trends Commun Inf Theory. 2006;2(3):155–239. doi: 10.1561/0100000006
[20] Picard E. Sur un théoréme général relatif aux équations intégrales de premiére espéce et sur quelques problémes de physique mathématique. Rendiconti del Circolo Matematico di Palermo. 2010;29(1):79–97. doi: 10.1007/BF03014061
[21] Sadek RA. Svd based image processing applications: state of the art, contributions and research challenges. Int J Adv Comput Sci Appl. 2012;3(7). doi: 10.14569/IJACSA.2012.030703
[22] Incropera F, DeWitt D, Bergman T, et al. Fundamentals of heat and mass transfer. Vol. 6, New York: John Wiley & Sons; 1996.
[23] Khandkar M, Khan J, Reynolds A, et al. Predicting residual thermal stresses in friction stir welded metals. J Mater Process Technol. 2006;174(1–3):195–203. doi: 10.1016/j.jmatprotec.2005.12.013
[24] Siegman A. How to (maybe) measure laser beam quality. In: Diode pumped solid state lasers: applications and issues. Washington, D.C., US: Optical Society of America; 1998. p. MQ1.